Supporting Information

Precise Molecular Design for B-N Modified Polycyclic Aromatic Hydrocarbon Toward Mechanochromic Material

Huanan Huang*[a], Ying Zhou[a], Yawei Wang[a], Xiaohua Cao[a], Chuan Han[a], Guochang Liu[a], Zhixiong Xu[a], Changchao Zhan[a], Huanan Hu[a], You Peng[a], Ping Yan[a], Dapeng Cao*[b]

a. School of Chemistry and Environmental Engineering; Jiangxi Province Engineering Research Center of Ecological Chemical Industry; Jiujiang Key Laboratory of Organosilicon Chemistry and Application, Jiujiang University, Jiujiang 332005, China.

b. State Key Laboratory of Organic-Inorganic Composites, Beijing University of Chemical Technology, Beijing, 100029, China

Contents

1. General Information……..…….....S2

2. Procedure for the Synthesis of Compounds 1-4……S3

3. General Procedure for the Synthesis of Compound 5..…..….....S3

4. General Procedure for the Synthesis of Compound 6...…..….....S3

5. Characterization Data for the New Compounds ……S4

6. TGA Studies of Compound 5……..……S5

7. UV-Vis and FL Studies of Compound 5……...……S5

8. X-ray Crystallographic Studies of Compound 5 and 6….……S9

9. DFT Calculations…….....S10

10. Reference……S17

11. Scanned NMR Spectra for the New Compounds…….……..S18

General Information. All operations involving air- and moisture-sensitive compounds were carried out under an atmosphere of dry argon by using a modified Schlenk line. All solvents were freshly distilled from Na or P_2O_5. The ^{1}H, ^{13}C, ^{11}B spectra were recorded on a 400 MHz NMR spectrometer. Chemical shifts are referenced against external $BF_3{\cdot}Et_2O$ (^{11}B) and tetramethylsilane (TMS). High-resolution mass spectra (HRMS) were obtained on a Varian QFT-ESI spectrometer. The UV-vis spectra were recorded on a RAYLEIGH UV-2100 spectrometer. Fluorescence spectra were performed on F-7000 FL fluorescence spectrophotometer. Solid-state Fluorescence spectra were performed on Edinburgh Instruments FS5 fluorescence spectrophotometer. Thermal gravimetric analysis (TGA) was recorded on a Labsysevo system (SETRAM, France) under nitrogen atmosphere at a heating rate of 10℃/min from 25℃ to 800℃. The temperature of degradation (T_d) was correlated to a 5% weight. The X-ray diffraction (XRD) patterns were examined on a Bruker D8 Focus diffractometer (Bruker, Germany). Incident X-ray radiation is Cu $K\alpha_1$ radiation (λ=1.5405 Å) and Cu $K\alpha_2$ radiation (λ=1.5444 Å). The typical step size for signal collection is 0.01°with duration of 0.1 s at each step. Microstructures of sample powders were analyzed using a field emission scanning electron microscope (SEM, Hitachi S4800, Japan). Cyclic voltammetry (CV) experiments were performed in dichloromethane solutions. All measurements were carried out at room temperature with a conventional three-electrode (the working electrode: glassy carbon electrode, the reference electrode: saturated calomel electrode (SCE), and a Pt wire as the counter electrode). Ferrocene/ferrocenium redox couple (Fc/Fc^+) was used as an internal reference for all measurements. The commercially available compound **5′** was purchased from Sigma-Aldrich. A suitable crystal was selected and on a SuperNova, Dual, Cu at zero, AtlasS2 diffractometer. The crystal was kept at 100.00(10) K during data collection using graphite-monochromated CuKα radiation (λ = 1.54184Å). CCDC numbers: 2004086 (for compound **5**), 2004088(for compound **6**).The structures were solved by use of SHELXTL program[S1]. Refinements were performed on F^2 anisotropically for all the non-hydrogen atoms by the full-matrix least-squaresmethod.

DFT calculation: Theoretical calculations were performed using the ORCA program packages [S2]. The geometries were optimized at the B3LYP/def2-SVP level. Time-dependent TD-DFT with PBE0 function and basis set def2-TZVPD were then performed to further analyze the dipole moment with the optimized structure[S3]. The electrostatic potential surface maps (ESP) of molecular for **5** and **5′** were obtained by DFT at B3LYP level. Ground state geometries of **5** and **5′** were directly selected from single crystal structures and were used as molecular models with restricted optimization. On the basis of this, the excited energies in singlet (S_n) and triplet states (T_n) were estimated through a combination of TD-DFT and B3LYP at the 6-311+G(p, d) level. Based on the results of theoretical calculation to elucidate the mechanisms of possible singlet-triplet intersystem crossings, in which the channels from S_1 to T_n are believed to share part of the same transition orbital compositions. Herein, energy

levels of the possible T_n states are considered to lie within the range of $ES_1 \pm 0.3$ eV.

Procedures for the Synthesis of Compounds 1-4

The compounds **1-4** were synthesized according to the previous works [S4].

General Procedure for the Synthesis of Compound 5

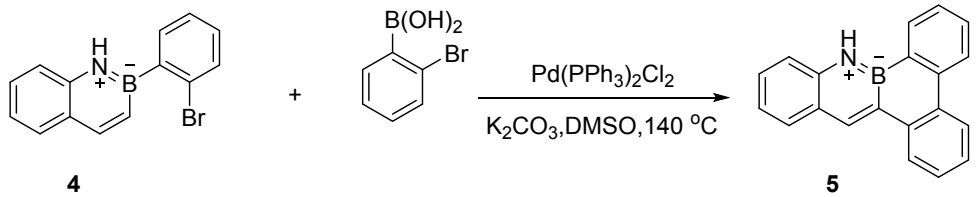

4 **5**

To a dried Schlenk flask, sealed with schlenk system, evacuated under vacuum, and purged with N_2 three times, charged with **4** (283 mg, 1 mmol), (2-bromophenyl)boronic acid (600 mg, 3 mmol), $Pd(PPh_3)_2Cl_2$ (70 mg, 10 mol %), DMSO 2 mL. The mixture was heated and stirred at 140°C for 18 h. The resulting mixture was successively washed with water (100 mL) and extracted twice with CH_2Cl_2 (60 mL). The combined organic layers were dried over Na_2SO_4. **5** was obtained as white powder (78%) by silica gel chromatography.

General Procedure for the Synthesis of Compound 6

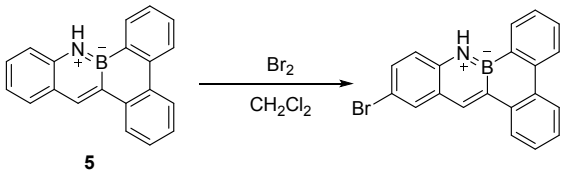

5

To a cooled solution (0 °C) of **5** (142 mg, 0.50 mmol) in CH_2Cl_2 (5 mL) was slowly added a solution of bromine (1M in CH_2Cl_2, 1.1 equivalents) diluted with CH_2Cl_2 (5 mL). After the addition, the mixture was stirred at 0 °C for 30 min, and then at room temperature for 2 h. The resulting mixture was evaporated to dryness to give the crude product, which was purified by flash column chromatography.

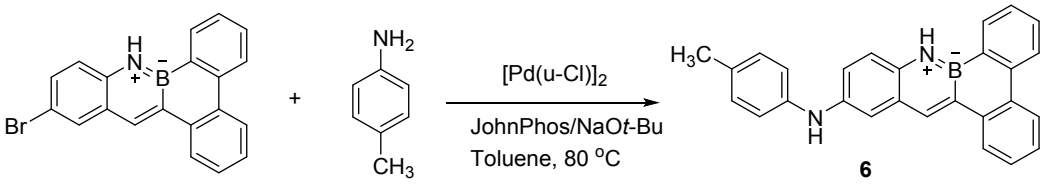

6

To an oven-dried schlenk tube with a stir bar was added **2** (0.5 mmol, 1 equiv) and p-toluidine (0.6 mmol, 1.2 equiv), Pd(μ-Cl) dimer (0.005 mmol, 1 mol %), JohnPhos (0.01 mmol, 2 mol%), and NaOt-Bu (0.7 mmol, 1.4 equiv). The tube was sealed with schlenk system, evacuated under vacuum, and purged with N_2 three times. Toluene (4 mL) was added; the resulting mixture was heated to 80°C and stirred 18 h. The reaction mixture was cooled to rt, and filtered over Celite. The solvent was removed in vacuo, and the product was purified by flash column chromatography on silica gel with hexanes and dichloromethane as the eluent.

Characterization Data for the New Compounds Reported in the Paper

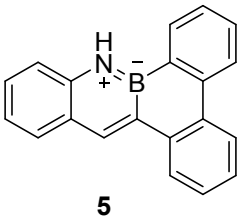

5

10H-benzo[e]dibenzo[3,4:5,6]borinino[1,2-b][1,2]azaborinine (5).

5 was obtained as white solid (78%). ^{1}H NMR (400 MHz, $CDCl_3$): δ 8.99 (1H, s), 8.71 (1H, s, *NH*), 8.26-8.53 (3H, m), 8.25 (1H, d, *J* = 4 Hz), 7.92 (1H, d, *J* = 4 Hz), 7.58-7.69(1H, m) 7.48-7.56(4H, m), 7.30-7.33 (1H, m,). ^{11}B NMR (128 MHz, $CDCl_3$): δ 29.74 . ^{13}C NMR (101 MHz, $CDCl_3$): δ141.31 (s, q uaternary-C), 139.54, 136.91, 133.93 (s, quaternary-C), 133.37 (s, quaternary-C), 130.64 (s,), 130.33, 1 29.83, 128.66, 127.16, 127.13, 126.14, 125.55(s, quaternary-C), 124.97, 124.15, 122.99, 121.18, 118.1 9. HR-MS (ESI): calcd. for $[M]^+$: 279.1219, found: 279.1181. The carbons attaching to boron were not observed.

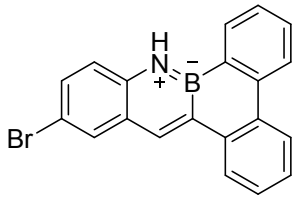

13-bromo-10H-benzo[e]dibenzo[3,4:5,6]borinino[1,2-b][1,2]azaborinine

^{1}H NMR (400 MHz, $CDCl_3$): δ 8.77 (1H, s), 8.58 (1H, s, *NH*), 8.40-8.46(3H, m), 8.16 (1H, d, *J* = 8 Hz), 7.98 (1H, d, *J* = 4 Hz), 7.65-7.71(1H, m) 7.48-7.59(4H, m), 7.34-7.37 (1H, m,). ^{13}C NMR (101 MHz, $CDCl_3$): δ141.34 (s, quaternary-C), 138.99(s, quaternary-C), 138.17, 137.56(s, quaternary-C), 135.49(s, quaternary-C), 133.60, 133.42, 132.18, 131.31, 130.93, 129.85, 127.64, 127.23, 127.00(s, quaternary-C), 126.28, 125.03, 124.23, 123.10, 119.73, 113.57(s, quaternary-C). HR-MS (ESI): calcd. for $[M]^+$: 357.0324, found: 357.0276.The carbons attaching to boron were not observed.

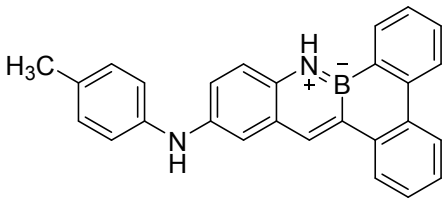

6

N-(p-tolyl)-10H-benzo[e]dibenzo[3,4:5,6]borinino[1,2-b][1,2]azaborinin-13-amine(6) was obtained as yellow solid (43%). ^{1}H NMR (400 MHz, $CDCl_3$): δ 8.83 (1H, s), 8.61 (1H, s, B-*NH*), 8.44-8.49 (3H, m), 8.21 (1H, d, *J* = 8 Hz), 7.64-7.70 (1H, m), 7.41-7.53(5H, m) 7.26-7.30(1H, m), 6.99-7.12 (4H, m), 5.6(1H, *NH*), 2.32(s, 3H, CH_3). ^{13}C NMR (101 MHz, $CDCl_3$): δ141.11 (s, quaternary-C, overlap), 136.22(s, overlap), 133.95(s, quaternary-C, overlap), 133.44(s, quaternary-C, overlap),130.43,

129.97, 129.74, 127.16, 127.09, 126.23(s, quaternary-C), 126.13, 124.99, 124.14, 123.01, 122.14, 119.01, 117.93, 117.67, 20.68. The carbons attaching to boron were not observed.

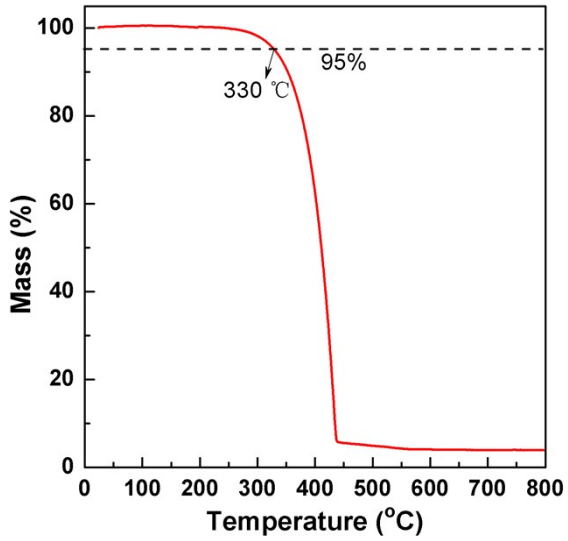

Figure S1. TGA graph of **5** (heating rate: 10℃/min under nitrogen flushing)

UV-Vis and FL Studies of Compound 5

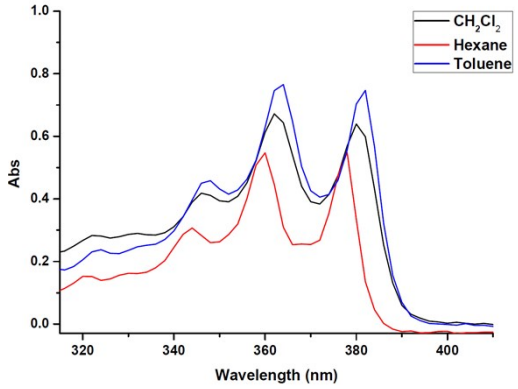

Figure S2. UV−vis spectra of **5** in CH_2Cl_2, n-hexane and toluene, respectively.

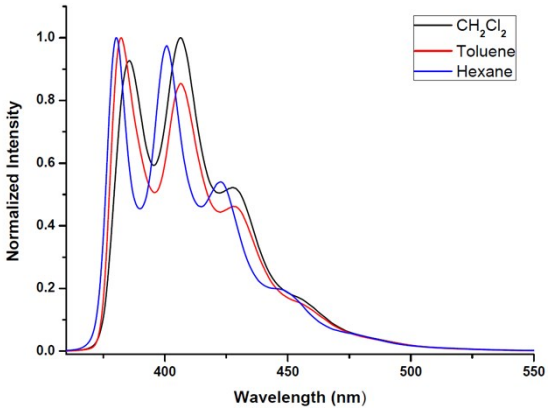

Figure S3. Normalized fluorescence emission spectra of **5** in CH_2Cl_2, *n*-hexane and toluene, respectively. All experiments upon excitation at the absorption maximum wavelengths.

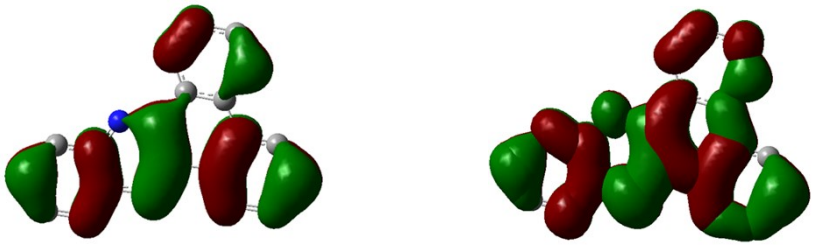

HOMO LUMO

Figure S4. The Calculated Frontier Orbitals of **5**

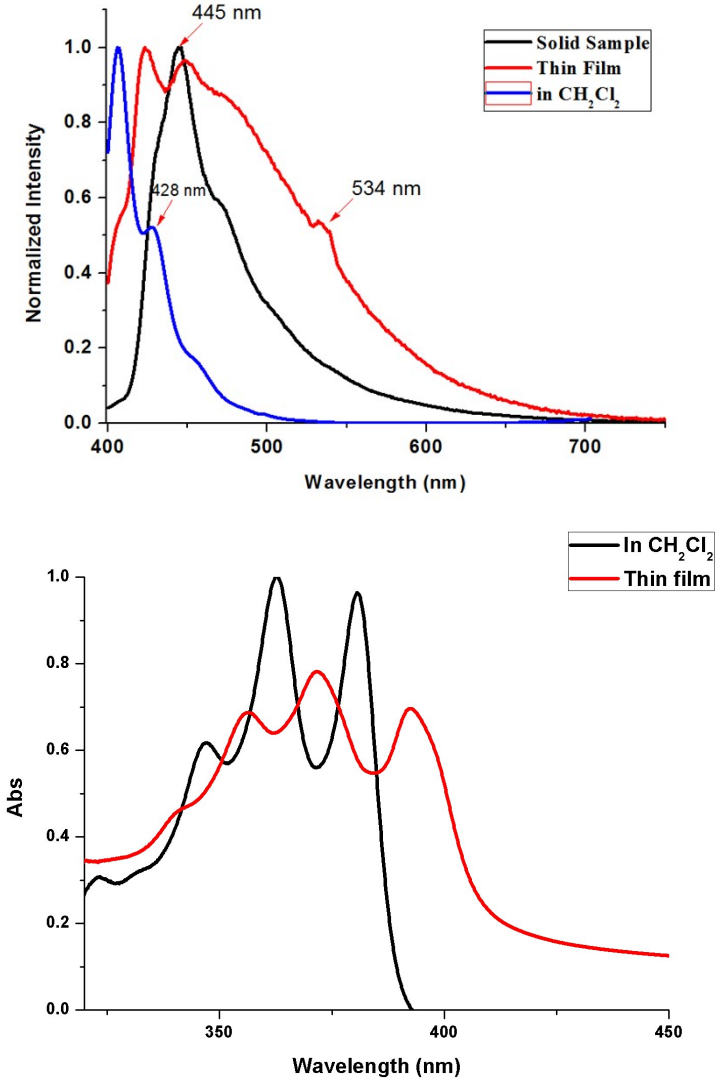

Figure S5. Up：Normalized fluorescence of **5** in different solid states, in CH_2Cl_2(blue line); solid powder (black line); thin film deposited via spin coating (red line)；Down：Absorption of compound **5** solved in CH_2Cl_2 (black line), as thin film deposited via spin coating (red line).

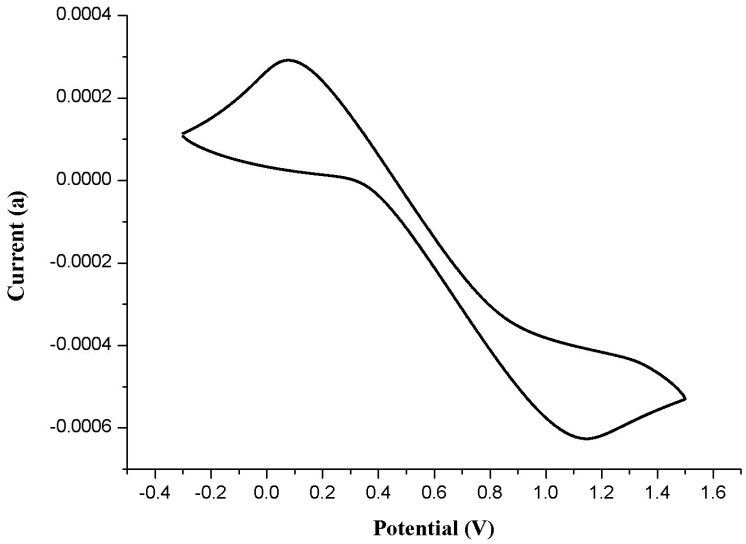

Figure S6. Cyclic voltammograms of Ferrocene measured in CH_2Cl_2 solution

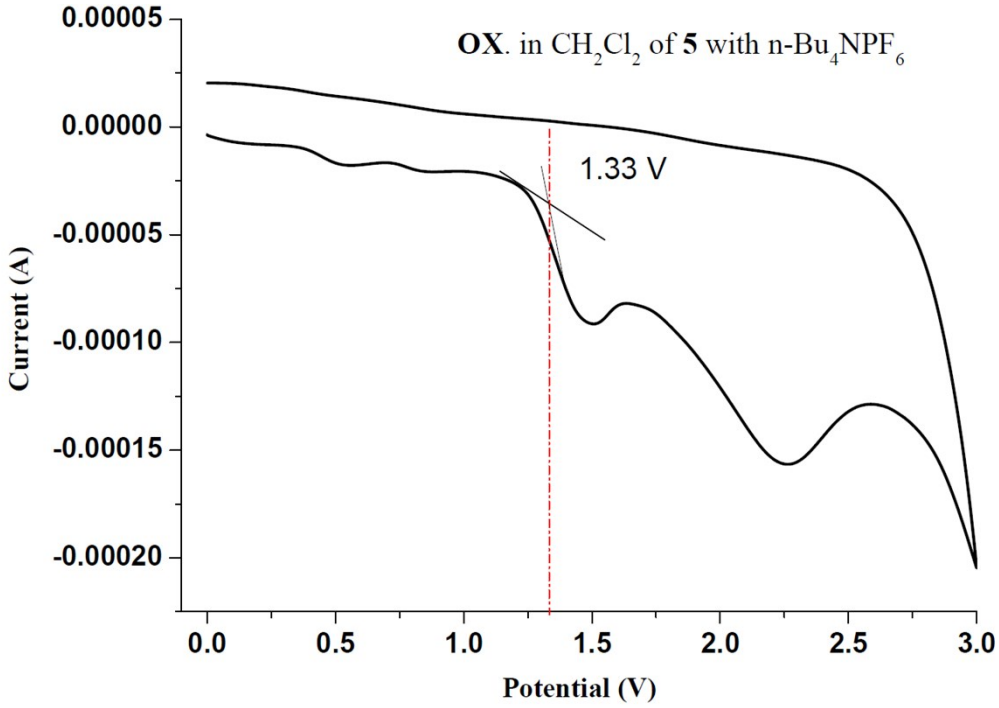

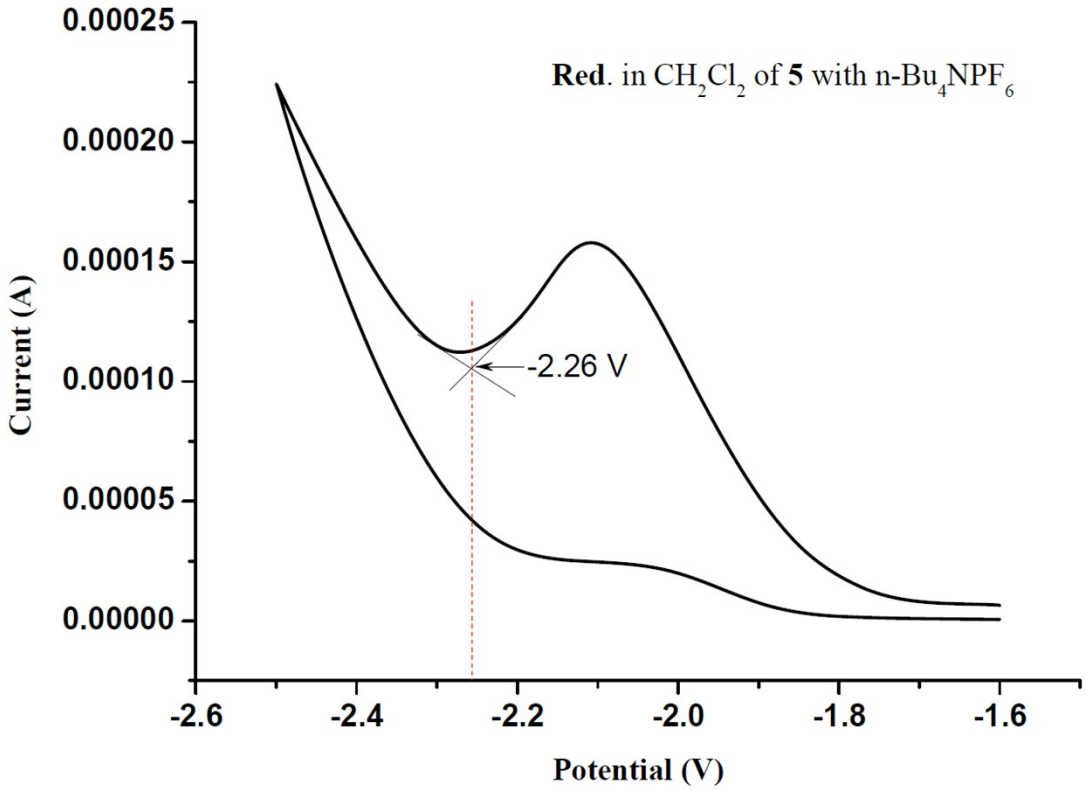

Figure S7. Cyclic voltammograms of 5 mM **5** measured in CH_2Cl_2 solution, containing 0.1 M $TBAPF_6$ as the supporting electrolyte at room temperature. Ferrocene/ferrocenium redox couple (Fc/Fc^+) was used as an internal reference and the scan rate at 100 mVs^{-1}.

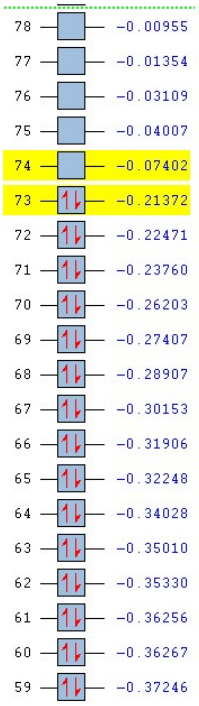

Figure S8. Calculated frontline orbital energy for 5

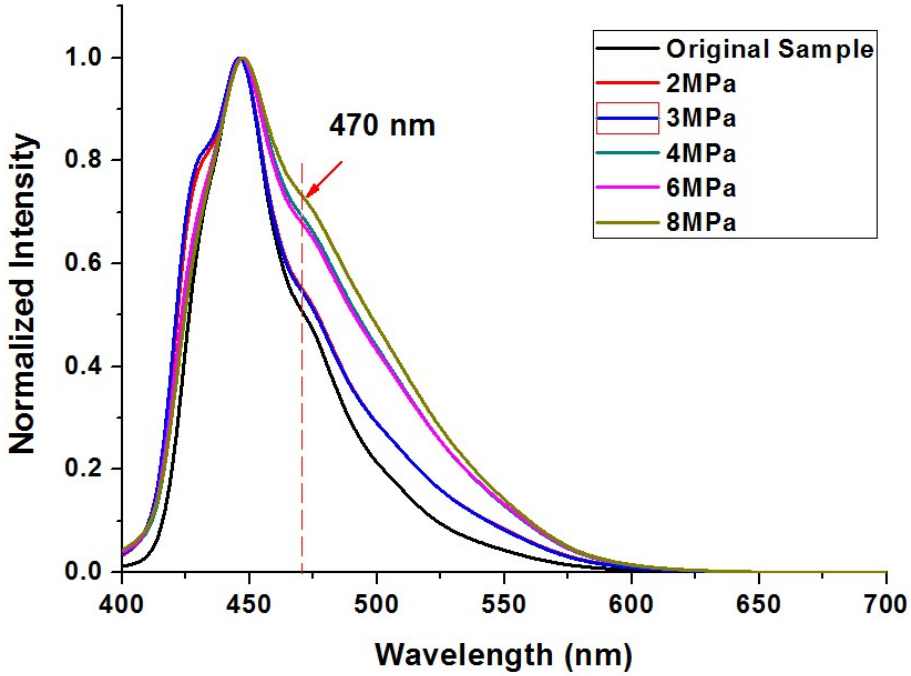

Figure S9. Quantitative experiments: The emission spectra of **5** obtained at different pressures

X-ray Crystallographic Studies of Compounds 5 and 6

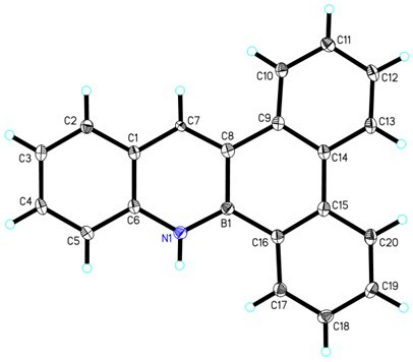

5

Figure 10. Molecule structure of **5**. Selected bond lengths (Å) and bond angles for **5**: B1-N1: 1.402(3)), B1-C8: 1.527(3), C6-N1: 1.403(2), N1-B1-C8: 117.58(18)°, N1-B1-C16 123.29(18)°, C16-B1-C8 119.06(17)°.

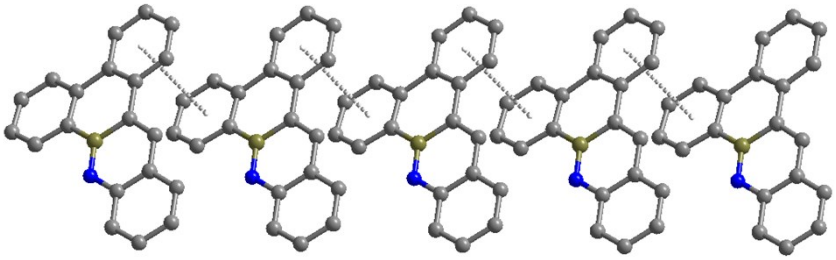

Figure S11. The π···π interactions between molecules along the b axis

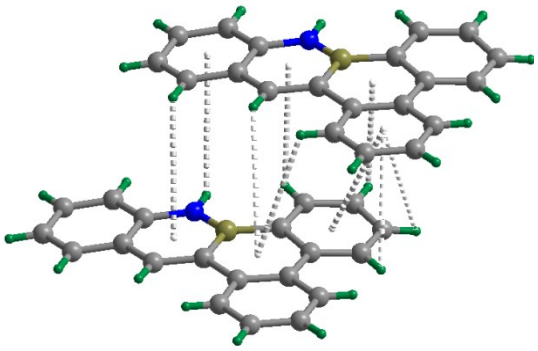

Figure S12. Intermolecular interactions of crystal **5**

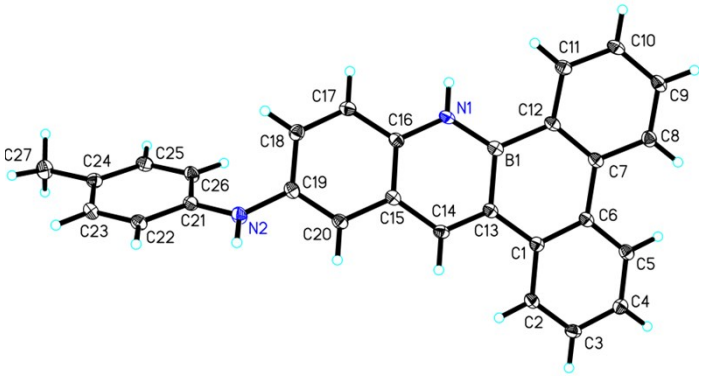

Figure S13. Molecular structure of **6**

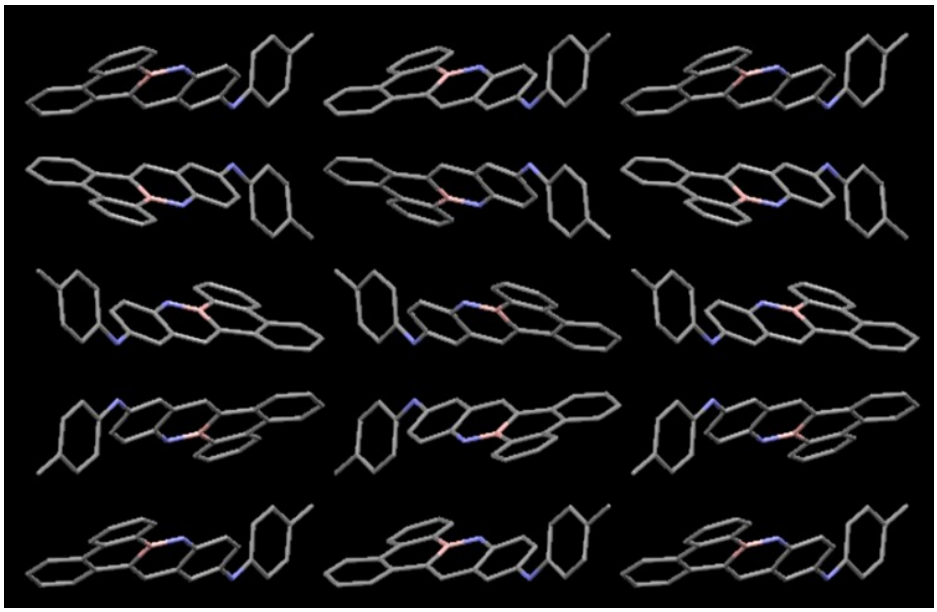

Figure S14. The stacking patterns of the referential compound **6**

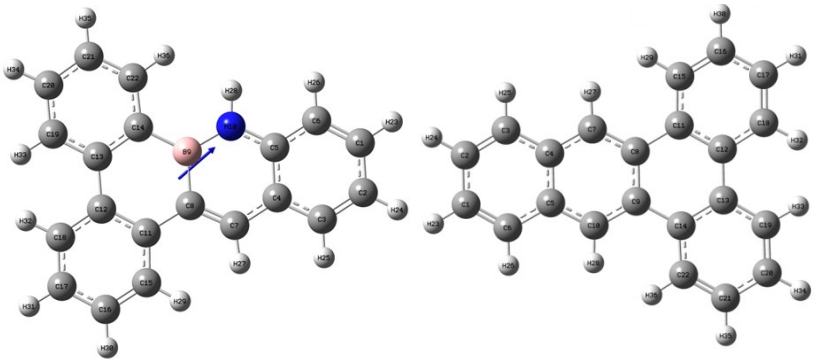

Figure S15. The dipole moment of **5** (left) and **5′** (right)

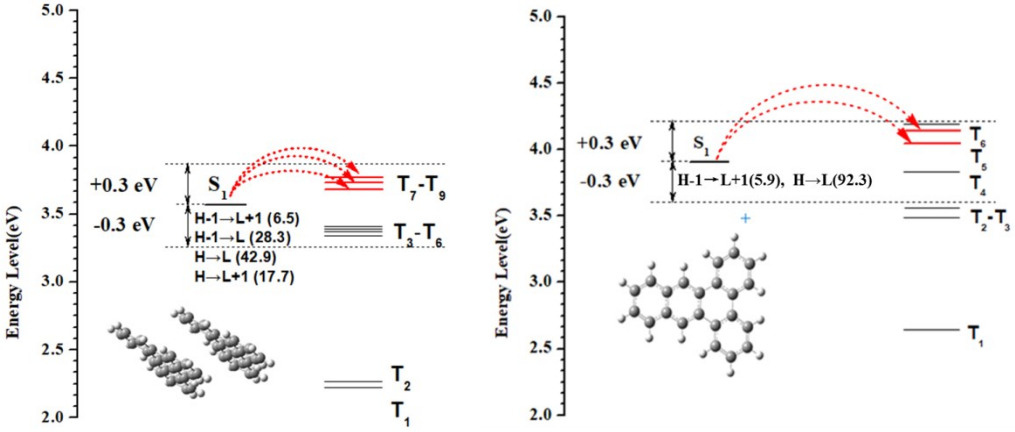

Figure S16. Energy level diagrams and possible ISC channels from excited singlet state (S_1) to excited triplet states (T_n) for the **5′** (left: dimer, right: isolate)

Table S1. Crystallographic data and structure refinement details for **5**.

	5
Empirical formula	$C_{20}H_{14}BN$
Formula weight	279.13
Temperature	100.00(10)
Radiation	CuKα (λ = 1.54184)
Crystal system, space group	monoclinic, C2/c
Unit cell dimensions	*a* = 20.7768(7) Å *b* = 5.8224(2) Å *c* = 24.2057(9)Å *α* = 90 deg. *β* = 110.115(4) deg. *γ* = 90 deg
Volume	2749.58(18) A^3
***Z*, Calculated density**	8, 1.349 g/m^3
Absorption coefficient	0.588 mm^{-1}
***F*(000)**	1168.0
Crystal size	0.15 × 0.13 × 0.12 mm
Theta range for data collection	7.78 to 147.068 deg
Limiting indices	-25 ⩽ h ⩽ 20, -7 ⩽ k ⩽ 5, -29 ⩽ l ⩽ 27
Reflections collected	4684
Independent reflections	2652 [Rint = 0.0198, Rsigma = 0.0224]

Data/restraints/parameters	2652/0/193
Goodness-of-fit on F^2	1.069
Final R indexes [I>=2σ (I)]	R_1 = 0.0616, wR_2 = 0.1760
Final R indexes [all data]	R_1 = 0.0650, wR_2 = 0.1792
Largest diff. peak/hole / e Å^{-3}	0.69/-0.65

Table S2. Crystallographic data and structure refinement details for **6**.

	6
Empirical formula	$C_{27}H_{21}BN_2$
Formula weight	384.27
Temperature	100.00(10)
Radiation	CuKα (λ = 1.54184)
Crystal system, space group	orthorhombic, C2/c
Unit cell dimensions	*a* = 18.5896(5) Å *b* = 8.4699(2)Å *c* = 24.5627(7)Å α = 90 deg. β = 90 deg. γ = 90 deg
Volume	3867.45(18) A^3
***Z*, Calculated density**	8, 1.32 g/m^3
Absorption coefficient	0.585 mm^{-1}
***F*(000)**	1616.0
Crystal size	0.13 × 0.12 × 0.11 mm
Theta range for data collection	7.198 to 147.306 deg
Limiting indices	-22 ⩽ h ⩽ 22, -10 ⩽ k ⩽ 8, -27⩽ l ⩽ 29
Reflections collected	9720
Independent reflections	3806 [Rint = 0.0408, Rsigma = 0.0444]
Data/restraints/parameters	3806/0/272
Goodness-of-fit on F^2	1.027
Final R indexes [I>=2σ (I)]	R_1 = 0.0526, wR_2 = 0.1283
Final R indexes [all data]	R_1 = 0.0725, wR_2 = 0.1437
Largest diff. peak/hole / e Å^{-3}	0.29/-0.32

Table S3. Cartesian coordinates for **5**

Center Number	Atomic Number	Atomic Type	Coordinates (Angstroms) X	Y	Z
1	6	0	5.165053	0.714678	0.000093
2	6	0	5.171583	-0.693062	-0.000247
3	6	0	3.972935	-1.382485	-0.000378
4	6	0	2.731043	-0.705316	-0.000179
5	6	0	2.741807	0.718689	0.000153
6	6	0	3.968086	1.411138	0.000291
7	6	0	1.486548	-1.417159	-0.000273

8	6	0	0.263444	-0.789522	-0.000029
9	5	0	0.261411	0.739915	0.000215
10	7	0	1.535398	1.385567	0.000319
11	6	0	-1.029640	-1.491170	0.000017
12	6	0	-2.252086	-0.749676	-0.000006
13	6	0	-2.283050	0.740960	-0.000062
14	6	0	-1.080767	1.501966	0.000139
15	6	0	-1.093950	-2.899891	0.000142
16	6	0	-2.296025	-3.588807	0.000190
17	6	0	-3.493028	-2.868106	0.000149
18	6	0	-3.458660	-1.481293	0.000074
19	6	0	-3.506518	1.445319	-0.000310
20	6	0	-3.552302	2.833786	-0.000307
21	6	0	-2.370718	3.581388	-0.000076
22	6	0	-1.157779	2.906822	0.000126
23	1	0	6.104006	1.261387	0.000196
24	1	0	6.113980	-1.232668	-0.000394
25	1	0	3.967252	-2.470040	-0.000629
26	1	0	3.963306	2.499280	0.000555
27	1	0	1.574060	-2.503140	-0.000572
28	1	0	1.610356	2.396738	0.000494
29	1	0	-0.172354	-3.472571	0.000264
30	1	0	-2.303085	-4.675479	0.000299
31	1	0	-4.449153	-3.384466	0.000189
32	1	0	-4.407944	-0.959999	0.000108
33	1	0	-4.451638	0.915878	-0.000525
34	1	0	-4.516321	3.336205	-0.000493
35	1	0	-2.403308	4.667577	-0.000093
36	1	0	-0.239851	3.493197	0.000232

Table S4. Cartesian coordinates for **5′**

Center Number	Atomic Number	Atomic Type	Coordinates (Angstroms) X	Y	Z
1	6	0	-5.138536	-0.711202	0.000013
2	6	0	-5.138577	0.710656	0.000157
3	6	0	-3.953314	1.405471	0.000196
4	6	0	-2.707063	0.715566	0.000085
5	6	0	-2.707016	-0.715961	-0.000055
6	6	0	-3.953223	-1.405943	-0.000086
7	6	0	-1.470364	1.386171	0.000113
8	6	0	-0.248079	0.719962	-0.000018
9	6	0	-0.247944	-0.720310	-0.000115
10	6	0	-1.470273	-1.386532	-0.000130
11	6	0	1.029467	1.449215	-0.000043
12	6	0	2.257407	0.735789	0.000084
13	6	0	2.257635	-0.735472	0.000125
14	6	0	1.029894	-1.449306	-0.000108
15	6	0	1.071382	2.860389	-0.000212
16	6	0	2.266232	3.559334	-0.000202
17	6	0	3.476477	2.856637	-0.000041
18	6	0	3.462134	1.472257	0.000083
19	6	0	3.462648	-1.471489	0.000331
20	6	0	3.477542	-2.855845	0.000218
21	6	0	2.267570	-3.558989	-0.000123
22	6	0	1.072452	-2.860508	-0.000273
23	1	0	-6.084398	-1.246066	-0.000017
24	1	0	-6.084471	1.245465	0.000235
25	1	0	-3.949357	2.493117	0.000307
26	1	0	-3.949193	-2.493587	-0.000190
27	1	0	-1.503393	2.469903	0.000281
28	1	0	-1.503383	-2.470225	-0.000157
29	1	0	0.149188	3.429059	-0.000392
30	1	0	2.258931	4.645805	-0.000340

	31	1	0	4.423563	3.389086	-0.000045
	32	1	0	4.413689	0.954602	0.000146
	33	1	0	4.414010	-0.953476	0.000602
	34	1	0	4.424832	-3.387929	0.000381
	35	1	0	2.260703	-4.645463	-0.000261
	36	1	0	0.150581	-3.429638	-0.000529

Table S5. The singlet and triplet excited state transition configurations of isolated **5** revealed by TD-DFT calculations. The matched excited states that contain the same orbital transition components of S_1 and $|S_1\text{-}T_n| < 0.3$ eV were highlighted in red.

5 (Isolated)	n-th	Energy (eV)	Transition configuration (%)
S_n	1	3.8025	H-1→L+2(2.3), H→L(93.6)
T_n	1	2.6843	H-2→L (2.5), H→L(85.9)
	2	3.3199	H-2→L(4.9), H-2→L+1(4.6), H-1→L(66.3), H-1→L+1(7.0), H→L(4.6)
	3	3.6340	H-3→L (5.7), H-2→L (47.8), H-2→L+1 (2.1), H-2→L+3 (2.9), H-1→L+1(16.8), H-1→L+3(3.1), H→L+1(11.2)
	4	3.9889	H-5→L+2(2.2), H-4→L+4(2.3), H-2→L(10.5), H-2→L+1(7.9), H-2→L+2(2.9), H-1→L(19.0), H-1→L+1(16.9), H-1→L+3(2.6), H→L(4.6), H→L+2(20.4)
	5	4.1778	H-4→L (6.4), H-4→L+1 (9.0), H-3→L (3.4), H-3→L+4 (2.5), H-2→L+1 (2.7), H-2→L+2 (3.8), H-2→L+3 (7.0), H-1→L+4 (2.5), H→L+1(12.8), H→L+3(4.9), H→L+4(8.5),

Table S6. The singlet and triplet excited state transition configurations of **5** dimer revealed by TD-DFT calculations. The matched excited states that contain the same orbital transition components of S_1 and $|S_1\text{-}T_n| < 0.3$ eV were highlighted in red.

5 (dimer)	n-th	Energy (eV)	Transition configuration (%)
S_n	1	3.7333	H-2→L+1(2.7), H-1→L(36.1), H-1→L+1(10.0), H→L(22.4), H→L+1(23.5)
	1	2.6252	H-2→L(2.2), H-1→L(65.7), H-1→L+1(10.0), H→L+1(6.8)
	2	2.6716	H-4→L+1(3.2), H-2→L+1(7.0), H-1→L+1(2.2), H→L(10.0), H→L+1(63.6)
	3	3.2916	H-4→L+3(2.1), H-3→L+1(18.8), H-2→L(17.1), H-2→L+1(24.2),H-2→L+3(5.4), H→L+3(6.7),
	4	3.3217	H-5→L(2.8), H-5→L+2(2.2), H-3→L(34.1), H-3→L+2(6.4), H-2→L(9.5), H-2→L+1(11.1), H-

T_n			2→L+2(5.0), H-1→L+2(6.8),
	5	3.6426	H-6→L+1(6.7), H-4→L(8.9), H-4→L+1(37.2), H-4→L+7(2.0), H-3→L+1(4.7), H-3→L+3(2.4), H-2→L+3(4.3), H→L(2.1), H→L+2(2.2), H→L+3(9.3)
	6	3.669	H-7→L(4.4), H-5→L(44.5), H-5→L+1(6.9), H-5→L+6(2.9), H-3→L(3.3), H-3→L+2(5.9), H-2→L+2(3.9), H-1→L+1(9.0)
	7	3.9431	H-5→L(3.3), H-5→L+2(2.1), H-4→L+1(2.8), H-4→L+3(2.3), H-4→L+5(2.7), H-3→L(2.4), H-3→L+2(7.7), H-2→L(8.1), H-2→L+1(3.6), H-2→L+3(9.4), H-1→L(5.2), H-1→L+4(5.1), H→L(4.2), H→L+3(5.5), H→L+5(7.8)
	8	3.9649	H-5→L(4.8), H-5→L+4(2.1), H-4→L+1(4.4), H-4→L+3(2.1), H-3→L(5.4), H-3→L+2(3.7), H-3→L+3(3.6), H-2→L(2.6), H-2→L+1(11.4), H-2→L+2(7.9), H-1→L(3.5), H-1→L+2(2.3), H-1→L+4(6.8), H→L+1(5.0), H→L+5(7.5)
	9	4.1579	H-6→L(6.7), H-6→L+1(13.2), H-4→L+1(2.5), H-4→L+7(2.1), H-2→L(2.5), H-2→L+5(5.6), H→L(10.5), H→L+2(4.3), H→L+3(17.6), H→L+4(2.6)

Table S7. The singlet and triplet excited state transition configurations of isolated **5′** revealed by TD-DFT calculations. The matched excited states that contain the same orbital transition components of S_1 and $|S_1-T_n| < 0.3$ eV were highlighted in red.

5′ (Isolated)	n-th	Energy (eV)	Transition configuration (%)
S_n	1	3.9054	H-1→L+1(5.9), H→L(92.3)
T_n	1	2.6463	H-3→L+3 (2.2), H-2→L(3.2), H-1→L+1(5.4), H→L(82.2)
	2	3.4906	H-1→L(58.8), H→L+1(29.6)
	3	3.5683	H-5→L+6 (2.7), H-3→L (5.2), H-2→L(11.9), H-2→L+2 (36.0), H-1→L+1(5.7), H→L+2(27.0), H→L+3(5.4)
	4	3.8376	H-1→L(30.2), H→L+1(60.4),
	5	4.0129	H-4→L +4(2.3), H-3→L (2.5), H-3→L+2 (3.4), H-2→L (6.8), H-2→L+3 (2.7), H-1→L+1 (58.0), H→L+3(6.5), H→L+2(12.9)
	6	4.1589	H-6→L (5.3), H-5→L+1 (2.5), H-2→L(17.6), H-2→L+2 (11.8), H-2→L+5(2.2), H→L(3.9), H→L+2(5.8), H→L+3(25.9), H→L+5(2.9)
	7	4.1945	H-4→L+2 (10.3), H-3→L+1 (2.9), H-3→L+4(2.3), H-2→L+1 (13.6), H-2→L+4(6.4), H-1→L(2.4), H-1→L+2(52.5), H→L+1(2.1)
	8	4.4935	H-6→L(4.2), H-4→L+1 (6.6), H-3→L+2(9.6), H-2→L (4.8), H-2→L+2(20.0), H-2→L+3(8.8), H-1→L+1(18.4), H-1→L+4(8.4), H→L+2 (12.9), H→L+5(5.0)

Table S8. The singlet and triplet excited state transition configurations of dimer **5′** revealed by TD-DFT calculations. The matched excited states that contain the same orbital transition components of S_1

and $|S_1-T_n| < 0.3$ eV were highlighted in red.

5′ (dimer)	n-th	Energy (eV)	Transition configuration (%)
S_n	1	3.5649	H-1→L(28.3),H-1→L+1(6.5), H→L(42.9), H→L+1(17.7)
T_n	1	2.2540	H-1→L(27.3), H-1→L+1(13.1), H→L(37.1), H→L+1(9.3)
	2	2.2656	H-2→L+4(2.2), H-1→L(13.7), H-1→L+1(25.2), H→L(10.7), H→L+1(37.0)
	3	3.3375	H-3→L (5.7), H-3→L+1 (18.1), H-2→L(22.4), H-2→L+1 (8.7), H-1→L+4(3.2), H-1→L+5(5.1), H→L+2(2.3), H→L+2(7.1)
	4	3.3566	H-3→L(30.2), H-2→L+1(27.0), H-1→L+4(27.0), H→L+3(4.9), H→L+4(2.5), H→L+5(5.3)
	5	3.3880	H-5→L +2(14.2), H-5→L+3 (4.3), H-4→L+1 (3.0), H-4→L+3 (12.7), H-4→L+5 (5.0), H-3→L (4.2), H-2→L+3 (4.7), H-2→L+4(2.6), H-1→L+2(9.2), H→L+3(8.0), H→L+5(4.9)
	6	3.3897	H-5→L+1 (2.3), H-5→L+3 (17.1), H-5→L+5(3.3), H-4→L+2 (19.4), H-4→L+5(2.2), H-3→L+5(3.0), H-2→L+4(5.2), H-1→L+3(8.5), H-1→L+5(2.2), H→L+2(11.0)
	7	3.6877	H-3→L (6.5), H-2→L+1 (12.8), H-1→L(8.0), H-1→L+2 (3.0), H-1→L+4(17.1), H-1→L+5(2.2), H→L(2.0), H→L+1(6.6), H→L+3(4.4), H→L+4(12.8), H→L+4(10.3)
	8	3.7146	H-3→L(5.9), H-3→L+1 (8.0), H-2→L(9.6), H-1→L+1 (14.7), H-1→L+2(2.3), H-1→L+3(5.0), H-1→L+4(3.3), H-1→L+5(14.6), H→L (2.2), H→L+2(7.3), H→L+3(2.9), H→L+4(16.4), H→L+5(7.2)
	9	3.8248	H-7→L(6.5), H-6→L(2.6), H-6→L+1(3.7), H-3→L+2 (2.2), H-3→L+5(5.2), H-2→L+4(2.4), H-1→L+1(2.8), H-1→L+2(9.8), H-1→L+6 (8.0), H→L(2.6), H→L+3(8.6), H→L+5(2.3), H→L+6(5.0), H→L+7(4.4)
	10	3.8433	H-7→L+1(4.5), H-6→L(5.5), H-6→L+1(3.1), H-2→L+4(12.4), H-1→L+2(4.3), H-1→L+3(7.0), H-1→L+7(7.4), H→L+2(11.4), H→L+5 (4.3), H→L+6(5.4), H→L+7 (3.5)
	11	3.8940	H-5→L+1(9.1), H-4→L(11.0), H-4→L+1(7.9), H-3→L+1(2.4), H-2→L(3.0), H-2→L+4(11.3), H-1→L+7(4.9), H→L(3.3), H→L+6 (3.1), H→L+7(5.3)

Reference

S1 G. M. Sheldrick. SHELXS-90/96, Program for Structure Solution, *Acta. Crystallogr. Sect. A* **1990**, *46*, 467.

S2 F. Neese. Software update: the ORCA program system, version 4.0, doi:10.1002/wcms.1327

S3 (a) A. D. Becke. “Density-functional thermochemistry. III. The role of exact exchange,” *J. Chem. Phys*., 98 (1993) 5648-52; (b) C. Adamo and V. Barone, “Toward reliable density functional methods without adjustable parameters: The PBE0 model,” *J. Chem. Phys*., 110 (1999), 6158-69.

S4 (a) Y.-Y. Chen, X.-J. Zhang, H.-M. Yuan, W.-T. Wei, M. Yan. *Chem. Commun.*, **2013**,*49*, 10974; (b)H. N. Huang, Z. X. Pan, C. M. Cui, C*hem. Commun*., **2016**, *52*, 4227.

Scanned NMR Spectra of All New Compounds

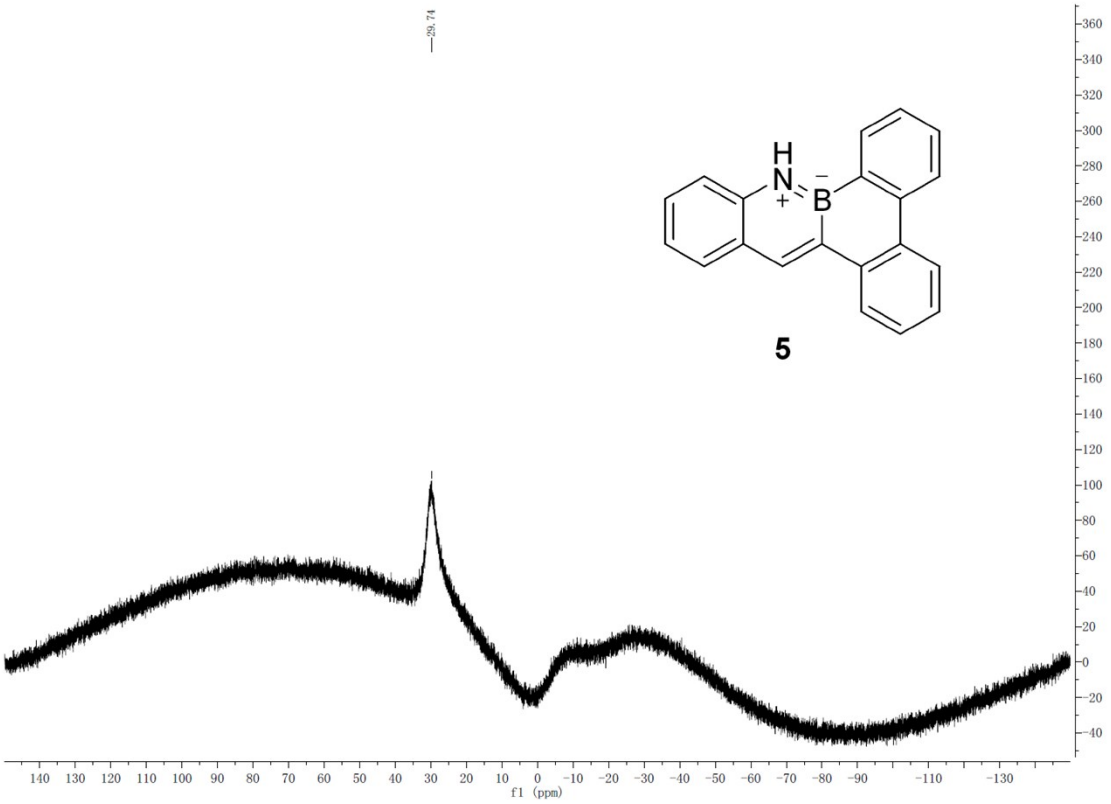
29.74
5
f1 (ppm)

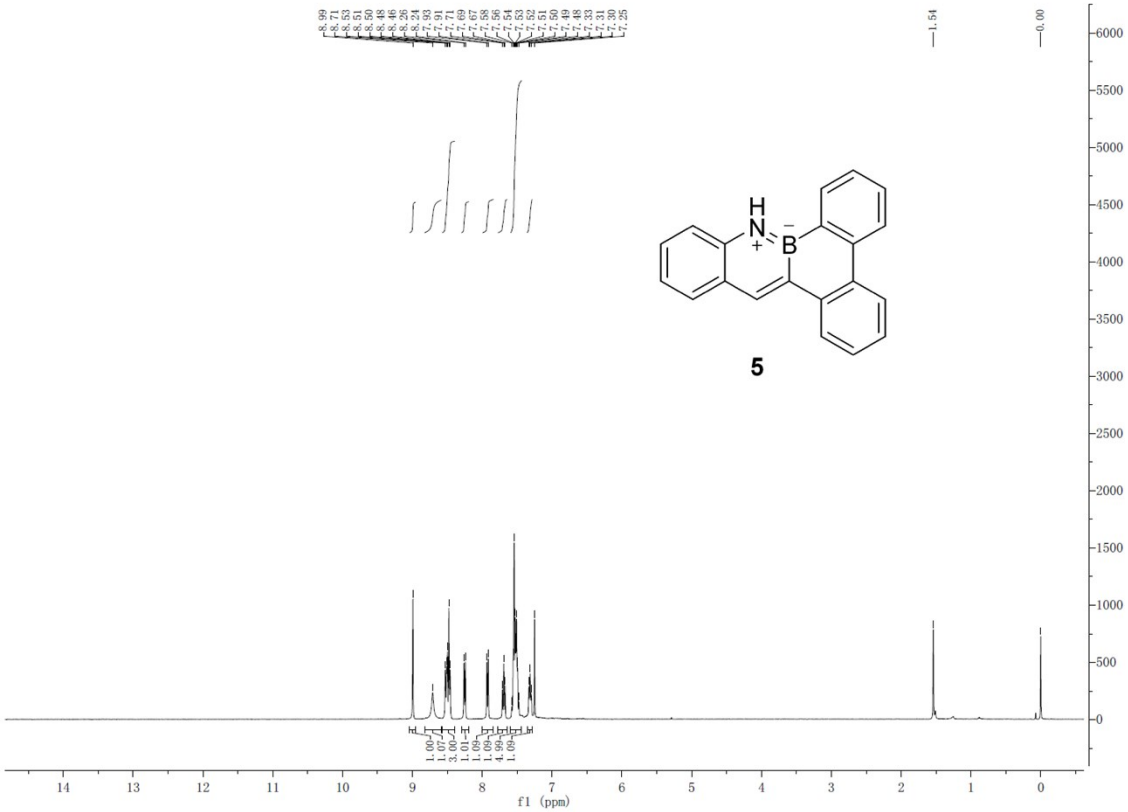
8.99
8.71
8.53
8.51
8.49
8.48
8.46
8.26
8.24
7.93
7.91
7.71
7.69
7.67
7.58
7.56
7.54
7.53
7.52
7.51
7.50
7.49
7.46
7.33
7.31
7.30
7.25
1.54
0.00
5
f1 (ppm)

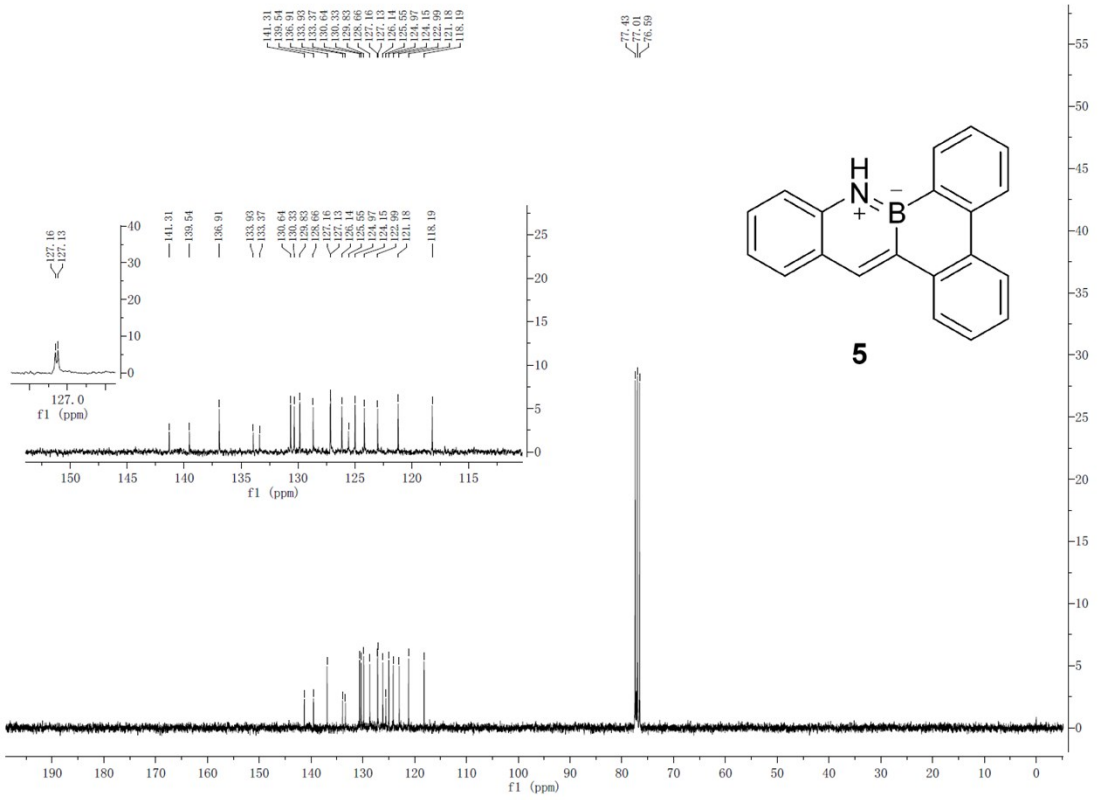
141.31
139.54
136.91
133.93
133.37
130.64
130.33
129.83
128.66
127.16
127.13
126.14
125.55
124.97
124.45
122.99
121.18
118.19
77.43
77.01
76.59
127.16
127.13
141.31
139.54
136.91
133.93
133.37
130.64
130.33
129.83
128.66
127.15
127.13
126.14
125.55
124.97
124.45
122.99
121.18
118.19
127.0
f1 (ppm)
150 145 140 135 130 125 120 115
f1 (ppm)
H
N
B
5
190 180 170 160 150 140 130 120 110 100 90 80 70 60 50 40 30 20 10 0
f1 (ppm)

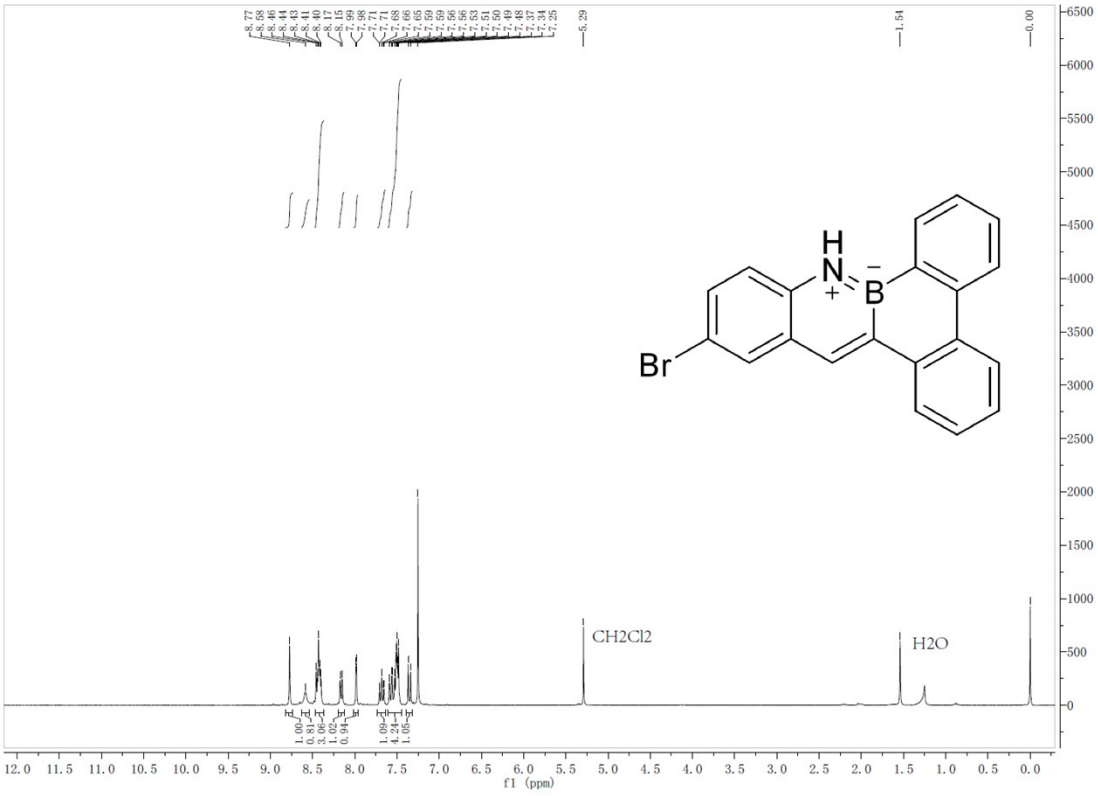
8.77
8.58
8.46
8.44
8.43
8.41
8.40
8.17
8.15
7.99
7.98
7.71
7.71
7.68
7.66
7.65
7.59
7.59
7.58
7.56
7.53
7.51
7.50
7.49
7.48
7.37
7.34
7.25
5.29
1.54
0.00
H
N
B
Br
CH2Cl2
H2O
1.00
0.81
3.06
1.02
0.94
1.00
4.24
1.05
12.0 11.5 11.0 10.5 10.0 9.5 9.0 8.5 8.0 7.5 7.0 6.5 6.0 5.5 5.0 4.5 4.0 3.5 3.0 2.5 2.0 1.5 1.0 0.5 0.0
f1 (ppm)

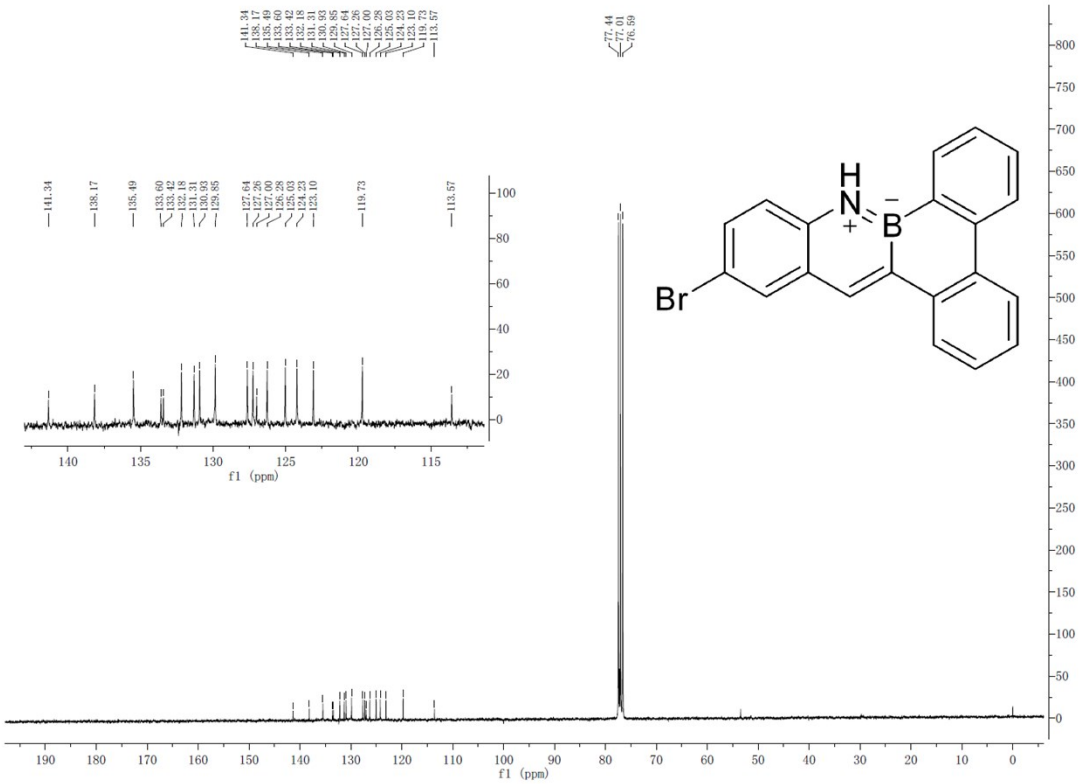
141.34
138.17
135.49
133.60
133.42
132.18
131.31
130.93
129.85
127.64
127.26
127.00
126.28
125.03
124.23
123.10
119.73
113.57
77.44
77.01
76.59
Br
f1 (ppm)

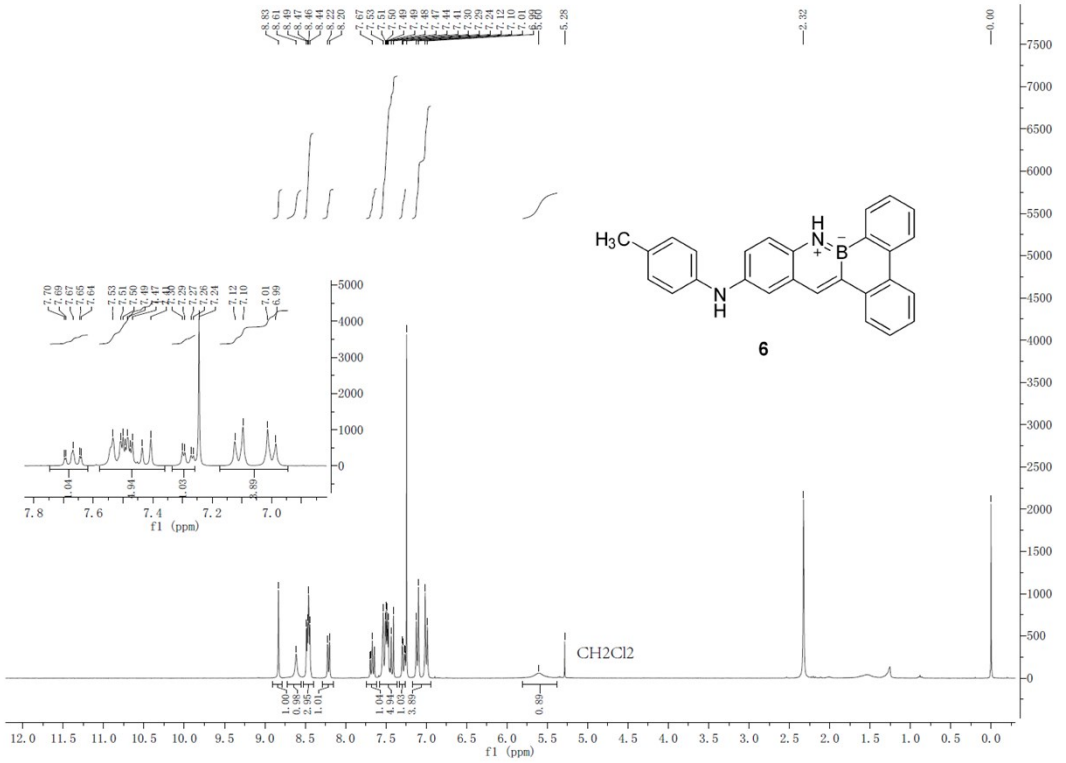
8.53
8.49
8.47
8.46
8.44
8.22
8.20
7.67
7.53
7.51
7.50
7.49
7.48
7.47
7.44
7.41
7.30
7.29
7.24
7.12
7.10
7.01
6.99
5.28
2.32
0.00
H3C
N
H
6
CH2Cl2
f1 (ppm)

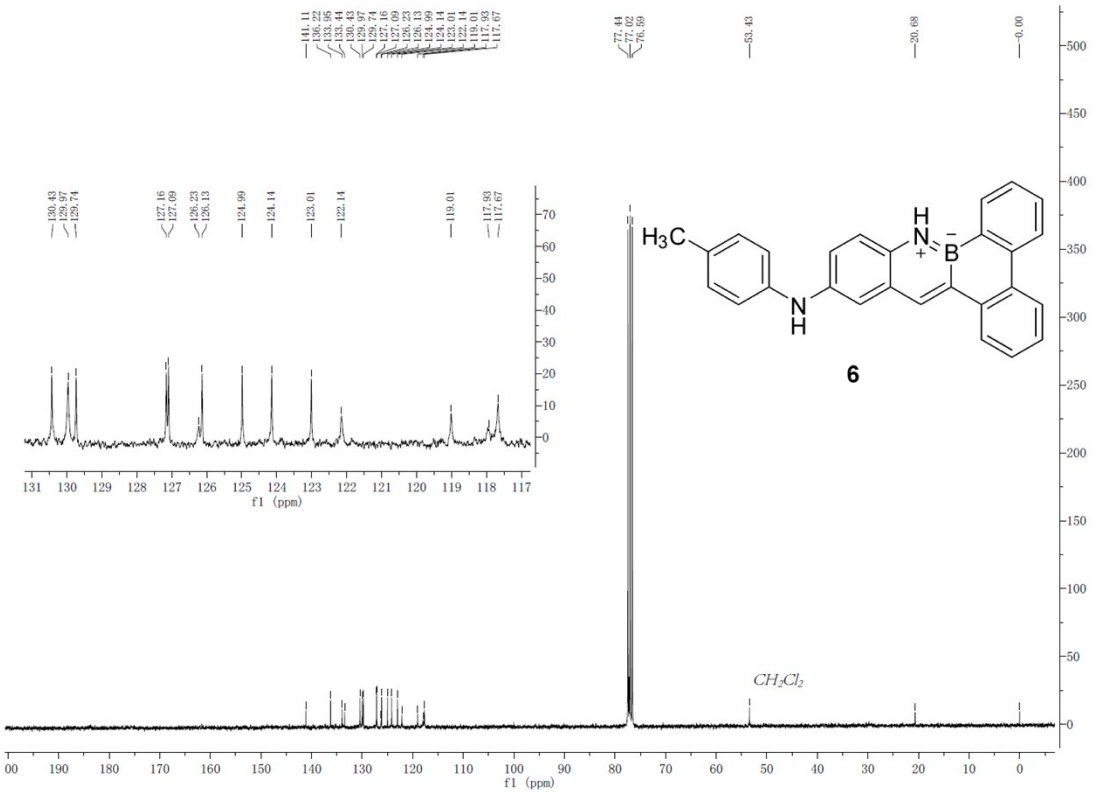
141.11
136.22
133.95
133.44
130.43
129.97
129.74
127.16
127.09
126.23
126.13
124.99
124.14
123.01
122.14
119.01
117.93
117.67
77.44
77.02
76.59
53.43
20.68
0.00
130.43
129.97
129.74
127.16
127.09
126.23
126.13
124.99
124.14
123.01
122.14
119.01
117.93
117.67
f1 (ppm)
f1 (ppm)
CH_2Cl_2
H3C
N
H
H
N
B
6